The current issue and full text archive of this journal is available on Emerald Insight at:
www.emeraldinsight.com/1757-9864.htm

Damage mechanism of giant orthogonal grid barrel vault under strong earthquake

Lin Qi
Airport College, Civil Aviation University of China, Tianjin, China, and
Wenbo Zhang, Ronglai Sun and Fang Liu
Civil Aviation University of China, Tianjin, China

Received 14 March 2019
Accepted 19 August 2019

Abstract

Purpose – Giant orthogonal grid barrel vault is generated by deleting members in the inessential force transfer path of the two-layer lattice barrel vault. Consisting of members in the essential transfer path only, giant orthogonal grid barrel vault is a new type of structure with clear mechanical behavior and efficient material utilization. The paper aims to discuss this issue.

Design/methodology/approach – The geometrical configuration of this structure is analyzed, and the geometrical modeling method is proposed. When necessary parameters are determined, such as the structural span, length, vault rise, longitudinal and lateral giant grid number and section height to top chord length ratio of the lattice member, the structure geometrical model can be generated.

Findings – Numerical models of giant orthogonal grid barrel vaults with different rise–span ratios are built using the member model that can simulate the pre-buckling and post-buckling behavior. So the possible member buckle-straighten process and the plastic hinge form–disappear process of the structure under strong earthquake can be simulated.

Originality/value – Seismic analysis results indicate that when the structure damages under strong earthquake there are a large number of buckling members and few endpoint plastic hinges in the structure. Dynamic damage of giant orthogonal grid barrel vault under strong earthquake is caused by buckling members that weaken the structural bearing capacity.

Keywords Modelling, Damage mechanism, Geometrical configuration, Giant orthogonal grid barrel vault, Strong earthquake

Paper type Research paper

Introduction

Lattice barrel vault has the advantages of both frame structure and shell structure. It is widely used for structure roofs of different shapes. In order to make lattice barrel vault span bigger area, the thickness or the layer number of the structure is usually need to increase. This would cause the increment of the structure self weight. Li pointed out that the structure layer increment made an ineffectual effort to improve the stability of the structure (Li *et al.*, 1998). Consisting of a large number of members, two-layer lattice barrel vault is a structure with high redundancy. Quite a few members that bear very small load are just for the sake of construction. By deleting the members on the inessential force transfer path of the two-layer lattice barrel vault a “hollow” lattice structure can be generated. This structure consists of giant lattice members which are generated by the remaining members. This structure can also be generated by replacing the solid web members of giant grid single-layer barrel vault with

Financial supports from Natural Science Foundation of Tianjin (18JCTPJC66200) and Scientific Research Program of Tianjin Education Commission (2018KJ244) are gratefully acknowledged.

the lattice members. The stiffness of lattice member is big, and the self weight of lattice member is obviously smaller than that of the solid web member of the same size. So the lattice member can be used for structural component of big size, and the structure with lattice member can be used to span bigger area.

Earthquake is one of the most frequent natural disasters. The losses of life and property due to earthquake are mainly caused by building collapse. Including the barrel vault with lattice members, seismic designs are needed for all types of structures which locate in the earthquake region. Study of dynamic damage mechanisms of long-span structures are carried out by scholars all over the world. Zhou *et al.* (2014) derived imperfect beam element model for reticulated shell member by supposing the initial curvature of members as half-wave sinusoids, they also studied the effect of member geometric imperfection on seismic performance of suspend-dome structure. Li and Xu (2014) studied the dynamic stability and failure probability of dome structures under stochastic seismic excitation. Liu and Ye proposed an optimization method for a single-layer spherical shell that collapses due to instability under earthquake action. The results show that the optimized structure is subject to ideal strength failure under earthquake action with clear warning signs prior to collapse (Liu and Ye, 2014). Mahmood and Morteza established six models of domes with different spans and same number of nodes and elements as well as loading conditions by finite element method to study the seismic behaviors. They proposed a formula of the structure natural period and response modification factor of Schwedler domes (Mahmood and Morteza, 2014). Sedeghi and Pour (2014) studied the site distance effect on seismic behavior of double layer barrel vaults, and some useful conclusions are obtained. Kang (2017) proposed a three-dimensional analysis method for determining the natural frequencies of shallow spherical domes with non-uniform thickness. This new method can also be used for refined analysis of unconventional long-span structures. Mousavi *et al.* (2015). investigated the effects of applying different buckling modes obtained by linearized eigenvalue buckling analysis as the initial imperfection for double domes free form space structures. They also suggested a generalized conformable imperfection mode method for the structural further dynamic analysis. Faghihmaleki *et al.* (2017) presented a probabilistic assessment and verify the effectiveness of seismic improvement schemes against earthquake, blast and progressive collapse.

Single-layer latticed domes composed of welded round pipes with different parameters are modeled, and the seismic responses of the domes with and without material fatigue are compared by the incremental dynamic analysis.

In this paper, the construction and damage mechanism of giant orthogonal grid barrel vault are studied. The giant orthogonal grid barrel vault is generated by replacing the solid web members of giant orthogonal grid single-layer barrel vault with the lattice members. In this structure, the lateral lattice members are orthogonal to the longitudinal lattice members. This is a new type of structure with efficient material utilization, and its mechanical behavior need to be further studied. It is the theoretical basis of the seismic design method to deeply study the objective laws of the dynamic responses and the damage mechanism of the giant orthogonal grid barrel vault under strong earthquake. Under the earthquake, the giant orthogonal grid barrel vault undergoes loading–unloading process repeatedly. It could cause the possible buckle-straighten processes of the structural members and the form–disappear processes of the plastic hinges. The member mechanical behavior and the structural bearing capacity are changing continuously. The refined member calculation model by which the continuous mechanical behavior changes of the member can be simulated should be founded. There are two main problems if members of giant orthogonal grid barrel vault are modeled by general beam element of the general finite element analysis program: the accuracy of the elastic–plastic element stiffness matrixes. By general finite element analysis program, the material constitutive relationships of the Gauss integral sections of the general beam element are used to calculate the element stiffness matrix. The elastic element stiffness matrix can be calculated correctly by this arithmetic if the member stays elastic. It is the end section of the member, which is not the Gauss integral section that first turns into plastic state commonly. Thus when the end section turns into plastic state, the element stiffness matrix calculated by general finite element analysis program is still elastic. Because of different loading history, material elastic–plastic constitutive relationships of different sections of the member are not the same, so it is not rational to calculate elastic–plastic element stiffness matrix based on the material constitutive relationship of the Gauss integral section. The simulation of the buckling members. If one structural member is modeled by a single general beam element of general finite element analysis program, buckling of the members cannot be simulated and the decrease of the member bearing capacity is caused by material yielding rather than member buckling. In this case, the member can bear the load that is bigger than the buckling critical load. Therefore the member bearing capacity is seriously overestimated. Buckling of the member can be simulated if one member is divided into more than one general beam element of general finite element analysis program. However, the post-buckling behaviors of the member and the plastic hinges forming in the end section and the central section cannot be simulated. How many general beam elements of general finite element analysis program one structural member should be divided into is also difficult to be appropriately determined.

To study the damage mechanism of giant orthogonal grid barrel vault under earthquakes, calculation model of the structure that tallies with the actual situation should be created. In this paper, refined member calculation model considering the buckling effect (Qi *et al.*, 2014) is used for the numerical model of giant orthogonal grid barrel vault. The bearing capacity change process of the structure under strong earthquake resulting from mechanism behavior change of the members is studied accordingly. Based on the objective laws of the structural dynamic responses, the damage mechanism of giant orthogonal grid barrel vault under strong earthquake is studied in this paper.

Geometrical model of the structure

Geometrical parameter

The structure of giant orthogonal grid barrel vault is illustrated in Figure 1. Space truss is used as the structural lattice member. One space truss consists of two top chords and one bottom chord. The top chords are connected by horizontal bars, and the top chords and the bottom chord

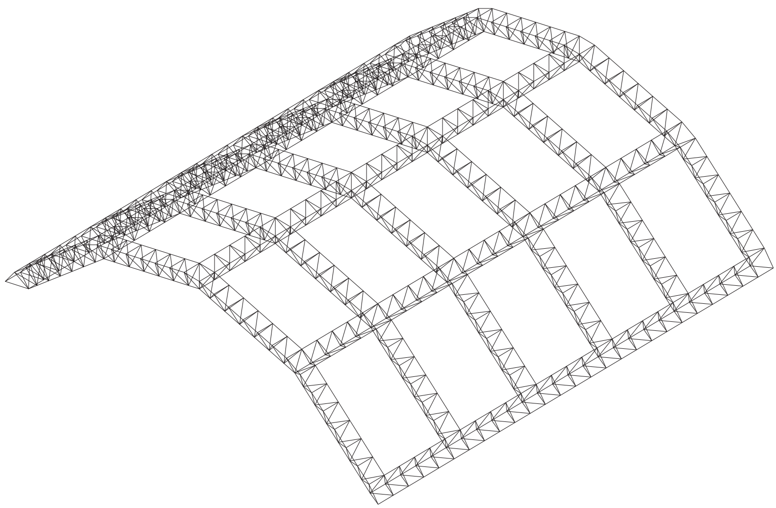

Figure 1.
Giant orthogonal grid barrel vault

are connected by web bars. Lattice members along the arch are connected by inverted square pyramid joints. The lattice member and the inverted square pyramid joint are shown in Figure 2.

The expressions of the structural geometrical parameters should be analyzed for the geometrical configuration of giant orthogonal grid barrel vault. The method of building the structural geometrical model based on the structural span, the length, the rise, longitudinal and lateral giant grid number and lattice member section height to top chord length ratio also needs to be developed. Vertical view of the structure is shown in Figure 3, and the plan view of the structure is shown in Figure 4.

In Figure 3, R is the curvature radius of the arch, H is the rise and S is the span. The relationship of is given as follow:

$$R^2 = \left(\frac{1}{2}S\right)^2 + (R-H)^2. \tag{1}$$

Based on Equation (1), the expression of R can be given as follow:

$$R = \frac{S^2 + 4H^2}{8H}. \tag{2}$$

As shown in Figure 3, 2θ is the central angle corresponding to one arch lattice member. N is the number of arch lattice members. So the central angle corresponding to the arch in Figure 3 is $2\theta N$. Based on the geometry theory, the expression of θ can be given as follow:

$$\theta = \frac{\arctan\frac{S}{2(R-H)}}{N}. \tag{3}$$

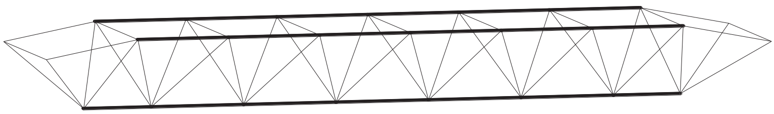

Figure 2.
Lattice member

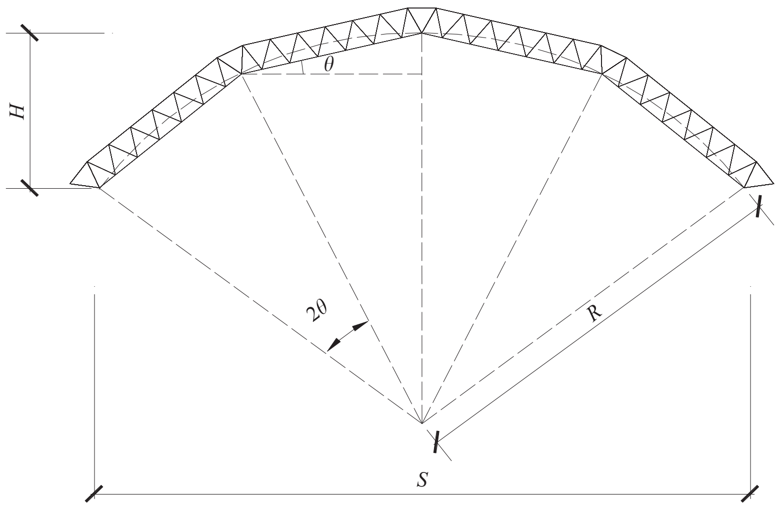

Figure 3.
Vertical view of the structure

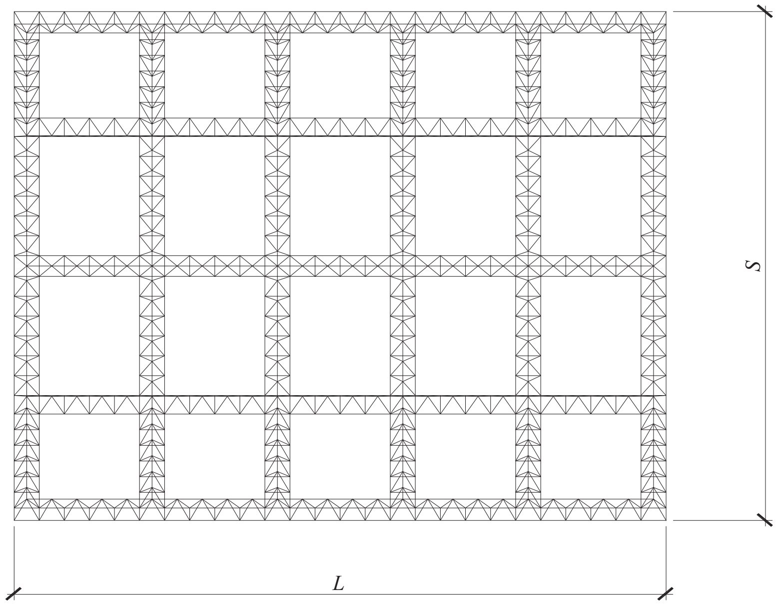

Figure 4.
Plan view of the structure

Geometrical parameters of one arch lattice member are shown in Figure 5. In Figure 5, A is the top length of the lattice member, and a is the length of one top chord in the lattice member. The relationship between A and a is given as follow:

$$A = na \tag{4}$$

where n is the number of top chords in one lattice member.

In Figure 5, h_1 is the section height of the lattice member. h_2 is the height of the inverted square pyramid joint. l_x is the length of the end bottom chord. Based on the geometry theory, the relationship of h_1, h_2, l_x and a is given as follow:

$$\left(l_x - \frac{1}{2}a\right)^2 + h_1^2 = \left(\frac{1}{2}a\right)^2 + h_2^2. \tag{5}$$

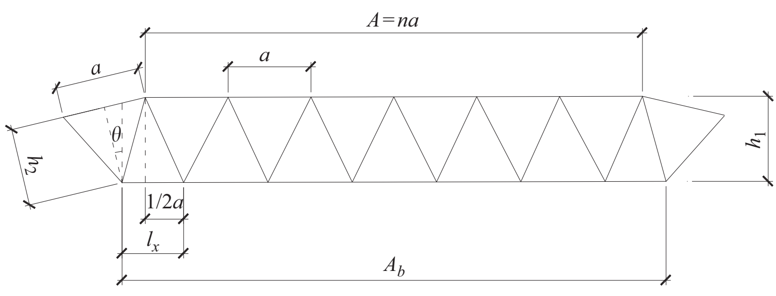

Figure 5.
Geometrical parameters of one arch lattice member

As shown in Figure 5, the angle between the joint median and the lattice member height is θ, and the relationship of θ, h_1 and h_2 is given as follow:

$$\left(\frac{1}{2}a\cdot\ \tan\ \theta+h_2\right)\cos\ \theta=h_1. \tag{6}$$

The bottom length of one lattice member is A_b. Based on the geometrical relationship in Figure 3, the expression for A_b can be given by:

$$A_b=2R\cdot\ \sin\ \theta. \tag{7}$$

Let $h_1=n_g a$, where n_g is the lattice member section height to top chord length ratio. Based on Equations (3), (5) and (6), the expression of the top chord length a is given as follow:

$$a=\frac{2\ \sin\ \theta\cdot\ \cos\ \theta}{1-2\cdot n_g a\cdot\ \sin\ \theta+n\cdot\ \cos\ \theta}\left(\frac{S^2}{8H}+0.5H\right). \tag{8}$$

Based on Equations (6) and (8), the expression of h_2 is given as follow:

$$h_2=n_g a(\cos\ \theta+\ \sin\ \theta\cdot\ \tan\ \theta)-0.5a\cdot\ \tan\ \theta. \tag{9}$$

Based on Equations (5), (6) and (8), the expression of the end bottom chord length l_x is given as follow:

$$l_x=\frac{1}{2}[2R\ \sin\ \theta-(n-1)a]. \tag{10}$$

Modeling processes

Modeling processes for giant orthogonal grid barrel vault are illustrated in Figure 6.

Detailed explanation of the processes is as follows:

(1) The structural span S, the structural rise H and the number of arch lattice member N should be first determined. Based on Equations (2), (3) and (8), the geometrical parameters of R, θ and a can be calculated. When the value of n_g is specified, h_1 can be determined by a and n_g, and h_2 also can be calculated by Equation (9). When the top node coordinate of the square pyramid joint at the end of an arch lattice member is specified, all of the nodal coordinates of the square pyramid joint can be determined based on h_2 and a. So the square pyramid joint at one end of this arch lattice member is constructed by connecting every node with solid web bars.

(2) The square pyramid joint at the other end of the lattice member can be constructed by rotating the completed square pyramid joint to an angle of 2θ along an arc with the center at the curvature center and the radius equal to R.

(3) The top chord line of the lattice member is constructed by connecting the bottom node of the inverted square pyramid. The bottom chord line of the lattice member is constructed by connecting the vertex of the inverted square pyramid.

(4) When the top chord line is separated at an equal distance of a, and the bottom chord line is separated at distances of a and l_x, the endpoints of top chords, bottom chords and web members are then determined. The top chords, bottom chords and web members of the giant lattice member can be constructed by connecting the endpoints.

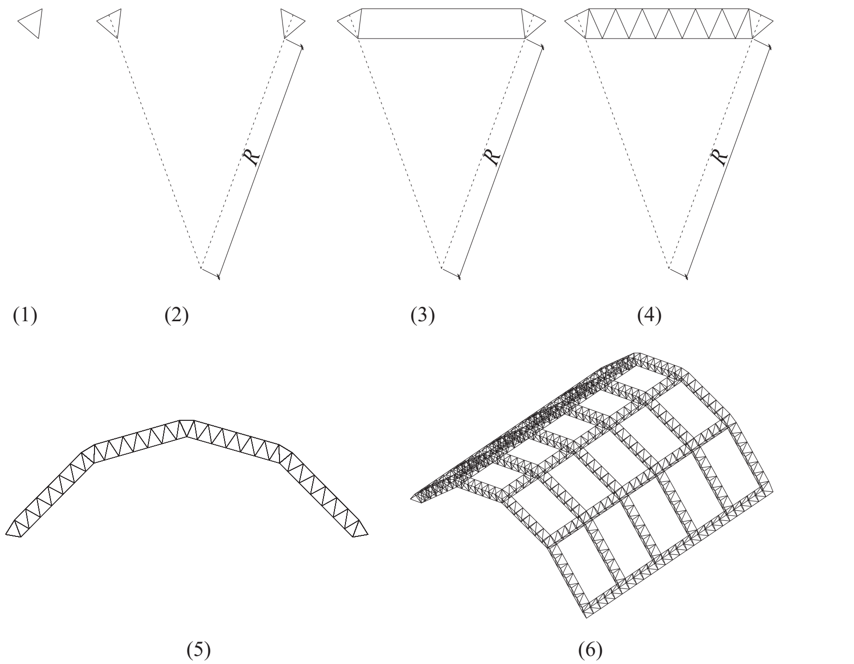

Figure 6.
Modeling processes

(5) Repeat this process from Step (2) to Step (4) and then a complete lattice arch can be constructed.

(6) Copy the lattice arch at an equal distance calculated by dividing the structural length by the longitudinal giant grid number. Then the top chord lines and the bottom chord lines of the longitudinal lattice members are constructed by connecting vertexes of the inverted square pyramid joints along the structural longitudinal direction. The endpoints of top chords, bottom chords and web members can be determined when the top chord lines and the bottom chord lines are equally separated. The top chords, bottom chords and web members of the longitudinal lattice members can be constructed by connecting the endpoints. The structure geometrical model is then constructed.

The geometrical modeling process of the giant orthogonal grid barrel vault is illustrated by Figure 7.

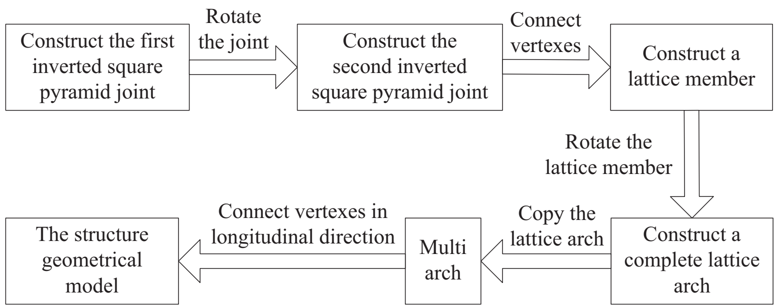

Figure 7.
The structure geometrical modeling process

Member buckling

Buckling is usually the key point of lattice structures. In this paper, member buckling is taken into consideration in the study of damage mechanism of giant orthogonal grid barrel vault under strong earthquake.

Member buckling prediction

Steel circular hollow sections are used as members of giant orthogonal grid barrel vault. Through extensive experiments, ISO summarize the instability equation of steel circular hollow section as follows (Steel Structures: Materials and Design, 1997):

$$I(\sigma_c, \sigma_{b1}, \sigma_{b2}) = \frac{\sigma_c}{N_c} + \frac{1}{N_b}\sqrt{\left(\frac{\xi_{m1}\sigma_{b1}}{1-\frac{\sigma_c}{N_{e1}}}\right)^2 + \left(\frac{\xi_{m2}\sigma_{b2}}{1-\frac{\sigma_c}{N_{e2}}}\right)^2}, \tag{11}$$

where $\sigma_c = N/\psi$ is the axial compressive stress; N and ψ are the axial force and the member cross section area, respectively; σ_{b1} and σ_{b2} are the maximum flexural stresses about the two main axes, respectively; $\sigma_{b1} = M_1/W_e$ and $\sigma_{b2} = M_2/W_e$, where W_e is elastic section modulus, and M_1 and M_2 are the maximum bending moments about the two main axes, respectively; ξ_{m1} and ξ_{m2} are reduction factors at the ends of the member, where $\xi_{m1} = \xi_{m2} = 0.85$; N_{e1} and N_{e2} are the Euler critical buckling stresses about the two axes, where $N_{e1} = N_{yc}/\lambda_1^2$, $N_{e2} = N_{yc}/\lambda_2^2$, $\lambda_1 = k_1L_1/\pi\rho\sqrt{N_{yc}/\chi}$, $\lambda_2 = k_2L_2/\pi\rho\sqrt{N_{yc}/\chi}$; L_1 and L_2 are the unsupported lengths of the member about the two axes; k_1 and k_2 are the effective length factors for L_1 and L_2; ρ is the radius of the section; χ is Young's modulus; N_c and N_b are the characteristic axial compression force and the characteristic bending force, respectively, and they are given by:

$$N_c = \begin{cases} (1.0-0.28\lambda^2)N_{yc} & \lambda \leqslant 1.34 \\ \frac{0.89282978}{\lambda^2}N_{yc} & \lambda > 1.34 \end{cases}, \tag{12}$$

$$N_b = \begin{cases} \frac{W_P}{W_e}\sigma_s & \frac{\sigma_s\phi}{\chi t} \leqslant 0.0517 \\ \left(1.133386-2.58\frac{\sigma_s\phi}{\chi t}\right)\frac{W_P}{W_e}\sigma_s & 0.0517 < \frac{\sigma_s\phi}{\chi t} \leqslant 0.1034 \\ \left(0.945198-0.76\frac{\sigma_s\phi}{\chi t}\right)\frac{W_P}{W_e}\sigma_s & 0.1034 < \frac{\sigma_s\phi}{\chi t} \leqslant \frac{120\sigma_s}{\chi} \end{cases}, \tag{13}$$

where N_{yc} is given by:

$$N_{yc} = \begin{cases} \sigma_s & 5\frac{\sigma_s\phi}{\chi t} \leqslant 0.170 \\ \left(1.04654873-0.27381606\frac{5\frac{\sigma_s\phi}{\chi t}}{3\chi t}\right)\sigma_s & 0.170 < 5\frac{\sigma_s\phi}{\chi t} \leqslant 1.911 \\ \frac{0.6\chi t}{\phi} & 5\frac{\sigma_s\phi}{\chi t} > 1.911 \end{cases}, \tag{14}$$

where σ_s is the yielding strength; t and ϕ are thickness and diameter of the member, respectively; $\lambda = \max(\lambda_1, \lambda_2)$; $W_P = [\phi^3-(\phi-2t)^3]/6$.

Generally when $I(\sigma_c, \sigma_{b1}, \sigma_{b2}) \geqslant 1.0$, member buckling is predicted. However, if the member is imposed with heavy bending moment but relative small axial compression force, it is possible that $I(\sigma_c, \sigma_{b1}, \sigma_{b2}) \geqslant 1.0$, which indicates a pseudo-buckling prediction. Hence, strength equation should be further employed, which is given by:

$$T(\sigma_c, \sigma_{b1}, \sigma_{b2}) = \frac{\sigma_c}{N_{yc}} + \frac{1}{N_b}\sqrt{\sigma_{b1}^2 + \sigma_{b2}^2} \tag{15}$$

Therefore, buckling criterion for steel circular hollow section member is defined as follows:

$$\begin{cases} I(\sigma_c, \sigma_{b1}, \sigma_{b2}) \geqslant 1.0 \\ T(\sigma_c, \sigma_{b1}, \sigma_{b2}) \leqslant 1.0. \end{cases} \tag{16}$$

When $I(\sigma_c, \sigma_{b1}, \sigma_{b2}) = 1.0$ and $T(\sigma_c, \sigma_{b1}, \sigma_{b2}) \leqslant 1.0$, the steel circular hollow section is under critical buckling status, and the critical axial compression force is given by:

$$N_{cr} = \sigma_c \psi. \tag{17}$$

Member buckling type

There are two possible buckling types of the compression members of lattice structures: Buckling Type I: the plastic hinge forms in the end section of the member, and slenderness ratio of the member gets bigger. This may cause the buckling of the member. The members of latticed structures bear concentrated forces at the nodes only, so it is the end section of the member where the stress is biggest. The buckling critical condition may not be satisfied when the plastic zone forms in the end section of the member. The plastic zone develops along with the increment of the load. When the plastic hinge forms in the end of the member and makes the slenderness ratio turn larger, the buckling critical condition gets easier to be met. Even a small increment of the external load may make the member buckling. The plastic zone or plastic hinge then forms in the central section of the buckled member as a combined action of both the axial compression force and the additional bending moment. Buckling Type II: the member bears compression axial force plenty big and the buckling critical condition is met without the plastic hinge forming in the end section. The plastic zone or plastic hinge then forms in the central section of the buckled member as a combined action of both the compression axial force and the additional bending moment.

Structural member model

Analysis model for pre-buckling member. Three nodes element with plastic hinge is employed to simulate the pre-buckling member. The incremental displacement at the end section of the member is comprised of the elastic part and the plastic part:

$$\Delta u = \Delta u^e + \Delta u^P, \tag{18}$$

where Δu, Δu^e and Δu^P are overall incremental displacement, elastic incremental displacement and plastic incremental displacement of the end section.

The transversal elastic displacement of the member can be expressed by quartic polynomial interpolation functions, the rotational displacement is the derivative of the transversal displacement with respect to the length; the axial displacement can be expressed by quadratic polynomial interpolation function; and the torsional displacement can be expressed by linear interpolation function. Naming the two ends of the member with "i" and "j", the equilibrium equation for the end "i" is given as follows:

$$\mathrm{P}_{mi} = \sum_{j=1}^{2}\sum_{n=1}^{6} K^{e}_{mi\ \ nj}\left(\mathrm{u}_{nj}-\mathrm{u}^{P}_{nj}\right), \tag{19}$$

where P_{mi} is the mth element of the force vector of the end "i"; $K^{e}_{mi\ \ nj}$ is the elastic tangent stiffness matrix; u_{nj} and u^{P}_{nj} are the nth element of the overall displacement vector and the plastic displacement vector of the end "j". The plastic displacement is accumulations of the incremental plastic displacement, and the incremental plastic displacement vector of the end "j" is given by:

$$\Delta u^{P}_{j} = \Delta\lambda_j \frac{\partial \Phi_j}{\partial S_j}, \tag{20}$$

where $\Delta\lambda_j$ is the scaling factor; $S_j = \mathrm{P}_j - \alpha_j$; P_j and α_j are vectors of the section force and the back stress; Φ_j is the yield surface function of the end "j", which is given by:

$$\Phi_j = \left(\frac{N_{xj}-\alpha_{Nxj}}{N_{xu}}\right)^2 + \left(\frac{T_{xj}-\alpha_{Txj}}{T_{xu}}\right)^2 + \left(\frac{M_{yj}-\alpha_{Myj}}{M_{yu}}\right)^2 + \left(\frac{M_{zj}-\alpha_{Mzj}}{M_{zu}}\right)^2 - 1, \tag{21}$$

where N_{xu}, T_{xu}, M_{yu} and M_{zu} represent the critical cross-sectional bearing capacities of the member, which are the axial force and three moments, respectively; N_{xj} is the axial force of the cross section at the end j; M_{yj} and M_{zj} are the bending moments about the local y and z directions of the cross section at the end j,respectively; M_{xj} is the torsion of section at the end j; α_{Nxj}, α_{Txj}, α_{Myj} and α_{Mzj} are the back stress components, respectively.

The cross section of the end j yields and the plastic hinge forms when $\Phi_j \geqslant 0$.

Analysis model for post-buckling member. Marshall model (Marshall *et al.*, 1977) is employed to simulate the post-buckling member. Marshall model is illustrated in Figure 8: A–F is the elastic tension phase; F–F′ is the hardening phase after yielding; A–B is the elastic compression phase; B–D is the buckling phase; and D–F is the tension phase. If the unloading occurs at the buckling phase of the envelop curve, i.e. point B′, C′ or D′, then the unloading path is depicted from the point where the unloading starts to the point F. When plasticity develops across the section under tension, the envelop curve shifts horizontally and the off-set distance equals the plastic deformation. In Figure 8, $\gamma = 0.02$; $\kappa = 0.28$; $\beta = 0.02$;

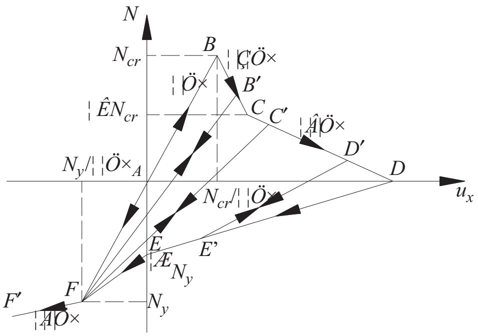

Figure 8.
Marshall model

$\zeta = \min(1.0, 5.8(tm/d)0.7/0.95)$; $\eta = 0.03+0.004l/\phi$, where l represents the length of the member. The ultimate axial force of the member is given by the following equation:

$$N_y = 0.95\sigma_s\psi. \tag{22}$$

Three nodes element with plastic hinge is initially employed to simulate the behavior of the member. At the end of each incremental step, the results are checked against Equation (16) to predict whether member buckling occurs. If the member is predicted to be stable, three nodes plastic hinge element will be employed continuously for the analysis; otherwise Marshall model will be employed instead. Three nodes element with plastic hinge is employed for the plastic hinge at the ends, while Marshall model is used for the plastic hinge at central.

Damage mechanism of the structure. The geometrical configuration and the force transfer path of giant orthogonal grid barrel vault are different with those of the normal barrel vault. Therefore, the damage mechanism of giant orthogonal grid barrel vault is also different with that of the normal barrel vault.

Take a giant orthogonal grid barrel vault with a span of 80 m, a length of 100 m and a rise–span ratio of 1/4 as an example. Its longitudinal giant grid number is 4, the lateral giant grid number is 4 and lattice member section height to top chord length ratio is 1.14. The geometrical model shown in Figure 9 is constructed based on the modeling method proposed in this paper. Steel circular hollow sections are used as the structural member, and the example structure is designed based on the Chinese Technical Specification for Space Frame Structures (JGJ7-2010) (China Architecture & Building 2010). The structure consists of Steel circular hollow sections of $\Phi 89\times 3.5$, $\Phi 114\times 3.5$, $\Phi 127\times 4.0$ and $\Phi 140\times 4.5$ of steel Q345. It is imposed surface load of 3.00 kN/m^2 and seismic excitation of El Centro wave with peak acceleration of 620 gal and duration of 12 s.

Numerical results indicate that buckling members appear in large numbers when giant orthogonal grid barrel vault undergoes strong earthquake. Almost all the buckling members behave as Buckling Type II. Time history of the buckling member number is illustrated in Figure 10. Based on Figure 10, it can be seen that there are a few buckling members before 4.78 s in the earthquake history. After 4.78 s the buckling members become more. After 9.10 s the number of buckling member increases rapidly. Subject to dynamic loads, the giant

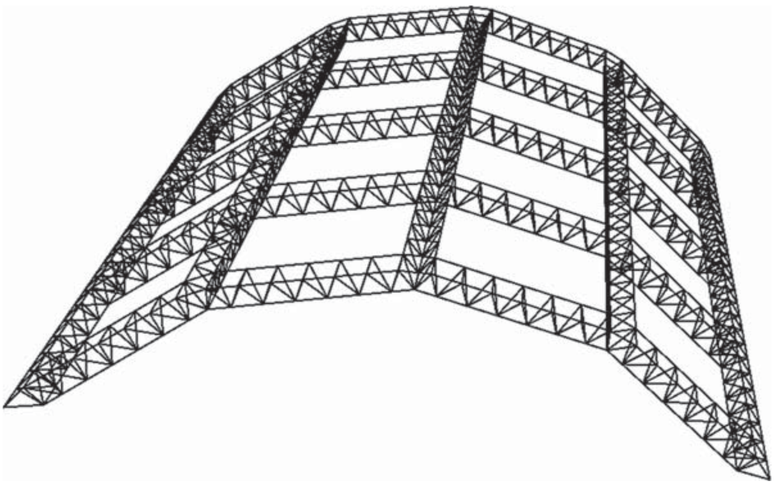

Figure 9.
The example giant orthogonal grid barrel vault

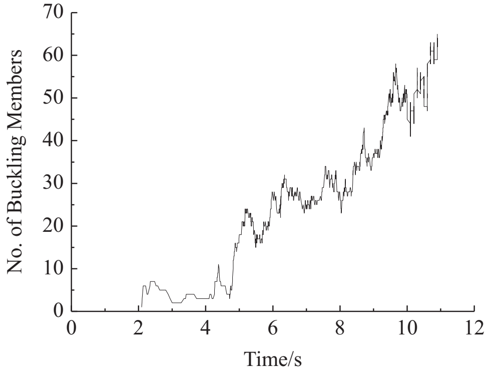

Figure 10.
Number of buckling members

orthogonal grid barrel vault undergoes loading–unloading process repeatedly, which leads to the possible buckle-straighten processes of the structural members. Capacity of the post-buckling member is different with that of the pre-buckling member. The number of structural buckling members changes continuously during the earthquake. So the mechanical behaviors of the members and the bearing capacity of the structure are changing continuously. The buckling members weaken the structural bearing capacity and cause the redistribution of the structural internal forces. At 10.90 s the buckling member number adds up to 65. Then the structure damages as it is unable to maintain the balance with the seismic action.

During the earthquake, the plastic hinge at the member endpoint is rarely generated in the structure. Only at 10.30 s, 1 endpoint plastic hinge is generated, and during 10.40–10.48 s, 2 endpoint plastic hinges are generated. After 10.48 s, the endpoint plastic hinges disappear under the seismic action. Until the damage happens, there are only 1 endpoint plastic hinge in the structure. Plastic hinges in the structure mainly result from the combined action of axial pressure and additional bending moment. They are commonly generated at the midpoint of the members.

Numerical models of five kinds of giant orthogonal grid barrel vault with uniform span of 80 m, uniform length of 100 m, and different rise–span ratios of 1/2, 1/3, 1/4, 1/5 and 1/6 are established, respectively for parameter analyses. Surface load of 3.00 kN/m^2 and seismic excitation of El Centro wave with peak acceleration of 900 gal and duration of 12.00 s are imposed. The number of buckling member and endpoint plastic hinge when the structure damages is presented in Table I.

Based on Table I, it can be deduced that the compression members of giant orthogonal grid barrel vault behave as Buckling Type II. When the structure damages, the number of buckling member is not in obvious relationship with the rise–span ratio. Rarely endpoint plastic hinges are generated in the structure during the seismic excitation. There are only 2 endpoint plastic hinges in the structure with rise–span ratio of 1/5 and 1 endpoint plastic hinge in the structure with rise–span ratio of 1/4 when the structural damage happens. In structures of other

Table I.
Numbers of buckling members and endpoint plastic hinges when structure damages

	Rise–span ratios				
Items	1/2	1/3	1/4	1/5	1/6
Number of buckling member	71	91	65	63	65
Number of endpoint plastic hinge	0	0	1	2	0
Damage time/s	9.43	11.00	10.90	11.21	10.62

rise–span ratios, there are no endpoint plastic hinge generated until they damage. Therefore, dynamic damage of giant orthogonal grid barrel vault under strong earthquake is mainly caused by buckling members which weaken the structural bearing capacity.

Conclusions

(1) In this paper, the geometrical configuration of giant orthogonal grid barrel vault is proposed by deleting the members on the inessential force transfer path of the two-layer lattice barrel vault. The structural lattice members are formed by remained solid web members. Giant orthogonal grid barrel vault is a new type of structure with clear mechanical behavior and efficient material utilization.

(2) The geometrical configuration of giant orthogonal grid barrel vault is analyzed, and the expressions of the structural geometrical parameters are also developed. The geometrical modeling method of the structure is proposed. When necessary parameters are input, such as the structural span, the length, the vault rise, longitudinal and lateral mega grid number, and lattice member section height to top chord length ratio, the complete structure geometrical model can be generated by this method.

(3) Numerical models of giant orthogonal grid barrel vaults with different rise–span ratios are built using the element model that can simulate the pre-buckling and post-buckling behavior of the structural member. By this refined element model, the possible member buckle-straighten process, the endpoint plastic hinge form–disappear process and the consequent bearing capacity changing process of the structure under strong earthquakes can be simulated.

(4) Seismic analysis results indicate that when giant orthogonal grid barrel vault damages under strong earthquake there are a large number of buckling members and few endpoint plastic hinges in the structure. Dynamic damage of giant orthogonal grid barrel vault under strong earthquake is caused by buckling members that weaken the structural bearing capacity.

References

Faghihmaleki, H., Najafi, E.K. and Aini, A.H. (2017), "Seismic rehabilitation effect in a steel moment frame subjected to tow critical loads", *International Journal of Structural Integrity*, Vol. 8 No. 1, pp. 25-34.

Kang, J.H. (2017), "Vibration analysis of shallow spherical domes with non-uniform thickness", *International Journal of Structural Stability and Dynamics*, Vol. 17 No. 2, pp. 1750016-1-1750016-18.

Li, J. and Xu, J. (2014), "Dynamic stability and failure probability analysis of dome structures under stochastic seismic excitation", *International Journal of Structural Stability and Dynamics*, Vol. 14 No. 5, pp. 1440001-1-1440001-22.

Li, Y.Y., Wang, B.B. and Liu, X.L. (1998), "Theoretical research of super-span barrel vaults", *Spatial Structures*, Vol. 4 No. 2, pp. 36-40.

Liu, W. and Ye, J. (2014), "Collapse optimization for domes under earthquake using a genetic simulated annealing algorithm", *Journal of Constructional Steel Research*, Vol. 97 No. 2, pp. 59-68.

Mahmood, Y. and Morteza, C. (2014), "Seismic behavior of single layer schwedler domes", *International Journal of Space Structures*, Vol. 29 No. 1, pp. 39-48.

Marshall, P.W., Gates, W.E. and Anagnostopoulos, S. (1977), "Inelastic dynamic analysis of tubular offshore structures", *Proceedings of Ninth Annual Offshore Technology Conference*, *Houston, TX*, pp. 235-246.

Mousavi, M.A., Abedi, K. and Chenaghlou, M. (2015), "Imperfection sensitivity analysis of double domes free form space structures", *International Journal of Structural Stability and Dynamics*, Vol. 15 No. 4, pp. 1450067-1-1450067-23.

Qi, L., Shao, Y.H., Huang, Z.W. and Huang, X. (2014), "Dynamic damage criterion and damage mode for single layer lattice shell", *Journal of Constructional Steel Research*, Vol. 99 No. 8, pp. 102-110.

Sedeghi, A. and Pour, S.S. (2014), "Site distance effect on seismic behavior of double layer barrel vaults", *International Journal of Space Structures*, Vol. 29 No. 3, pp. 137-144.

Steel Structures: Materials and Design (1997), *Specification for the Design and Construction of Steel Structures ISO10721-1*, International Standards Organization, Geneva.

Zhou, Z., Wu, J. and Meng, S. (2014), "Influence of member geometric imperfection on geometrically nonlinear buckling and seismic performance of suspend-dome structures", *International Journal of Structural Stability and Dynamics*, Vol. 14 No. 3, pp. 1350070-1-1350070-20.

Further reading

Ministry of Housing and Urban-Rural Construction of the People's Republic of China (2010), *Technical Specification for Space Frame Structures JGJ7-2010*, China Architecture & Building, Beijing.

Corresponding author
Lin Qi can be contacted at: qilin1208@vip.163.com